PROCEEDINGS OF SCIENCE

Collective effects in small collision systems from PYTHIA8 and EPOS4 simulations

C. D. Brandibur,* A. Danu, A. F. Dobrin and A. Manea

Institute of Space Science – INFLPR Subsidiary,
409 Atomistilor, Magurele, Romania
E-mail: diana.catalina.brandibur@cern.ch, andrea.danu@cern.ch, alexandru.florin.dobrin@cern.ch, alexandru.manea@cern.ch

Strong evidence exists that the quark–gluon plasma, a deconfined state of quarks and gluons created in heavy-ion collisions, exhibits a strong collective behavior. A similar collective behavior has also been observed in small collision systems. To study the origin of collectivity in small collision systems, the second order Fourier coefficient v_2 of inclusive charged particles and $\pi^{\pm}$, $K^{\pm}$, and $p+\overline{p}$ is measured in pp collisions at $\sqrt{s}$ = 13.6 TeV and p–Pb collisions at $\sqrt{s_{NN}}$ = 5.02 TeV simulated with different configurations of PYTHIA8 and EPOS4 event generators. Results obtained using the scalar product and cumulant methods are reported as a function of transverse momentum p_T in different multiplicity classes and as a function of charged-particle multiplicity N_{ch}, respectively. A strong dependence on N_{ch} is found for the second order two-particle cumulants, while the second order four-particle cumulants are consistent with zero. The v_2 of identified particles increases with the multiplicity class, being mass-ordered at low p_T for the 0–5% multiplicity class when a large $|\Delta\eta|$ gap is employed to suppress contributions from few-particle correlations.

42nd International Conference on High Energy Physics (ICHEP2024)
18-24 July 2024
Prague, Czech Republic

*Speaker

PoS(ICHEP2024)583

1. Introduction

The observed collective behaviour of the produced particles in pp [1], p–Pb [2], and Pb–Pb [3] collisions at the Large Hadron Collider through measurements of two- and multi-particle azimuthal correlations is extensively studied to characterize the properties of the medium created in such collisions. While measurements of the harmonic coefficients v_n in a Fourier decomposition of the azimuthal distribution of particles [4] compared with hydrodynamic models have revealed that the quark–gluon plasma created in heavy-ion collisions is the most perfect fluid, the origin of the collective effects in small collision systems still needs to be understood. The initial observation of collectivity in small collision systems was the appearance of a near-side ridge (i.e., elongated structure at $\Delta\varphi \sim 0$ in the two-particle correlation function vs. the difference in pseudorapidity, $\Delta\eta$, and azimuth, $\Delta\varphi$) in high-multiplicity pp and p–Pb collisions [1, 2]. Further studies of identified particle v_2 showed a mass ordering at low transverse momentum, p_{T}, followed by a crossing between meson and baryon v_2 and then a grouping based on particle type at intermediate p_{T} [5, 6].

The emergence of collective effects in pp collisions at $\sqrt{s}$ = 13.6 TeV and p–Pb collisions at $\sqrt{s_{\mathrm{NN}}}$ = 5.02 TeV is studied using two Monte Carlo event generators, EPOS4 [7] and PYTHIA8 [8], through azimuthal correlations of inclusive and identified particles. The EPOS4 model introduces parallel scatterings and implements a “core-corona" picture coupled to a hadronic afterburner where soft processes are evolved hydrodynamically in the “core" region and hard processes are controlled by strings in the “corona" part. Color confinement fields (i.e., strings) are employed in PYTHIA to handle the hadronization [9]. In addition, new mechanisms that give rise to collective effects (e.g., Rope hadronization) [10] have been introduced. Two configurations, Monash tune [11] with color reconnection and Rope hadronization, are employed to generate pp collisions, while the recently implemented Angantyr model [12] is used in p–Pb simulations.

2. Methods

The v_2 of inclusive and identified particles is measured using the scalar product method [13]

$$v_2\{\mathrm{SP}\} = \frac{\langle \mathbf{u}_{2,\mathrm{k}} \mathbf{Q}_2^{*}/\mathrm{M} \rangle}{\sqrt{\langle \mathbf{Q}_2^{\mathrm{a}} \mathbf{Q}_2^{\mathrm{b}*}/(\mathrm{M^a M^b}) \rangle}}, \tag{1}$$

where $\mathbf{u}_{2,k}$ is the unit vector of the particle of interest (POI) k with x and y components $u^x_{2,k} = \cos(2\varphi_k)$ and $u^y_{2,k} = \sin(2\varphi_k)$, respectively, $\mathbf{Q}_2$ is the event flow vector defined as $Q^x_{2,i} = \sum_l \cos(2\varphi_i)$ and $Q^y_{2,i} = \sum_l \sin(2\varphi_i)$, and M is the event multiplicity. Each event is split into two independent subevents a and b determined by particles from different pseudorapidity intervals with multiplicities M^a and M^b. The $*$ represents the complex conjugate and the angle brackets denote an average over all particles and events. To suppress “nonflow" (i.e., contributions from short-range correlations such as resonances and jets), different pseudorapidity gaps $|\Delta\eta|$ between POIs and reference particles (RPs) used to determine $\mathbf{Q}_2$ are introduced. A $|\Delta\eta| > 1.0$ is employed by taking POIs and RPs from $-1.0 < \eta < -0.5$ and $0.5 < \eta < 1.0$, respectively. The nonflow is further reduced by choosing POIs and RPs from $|\eta| < 1$ and $3.0 < \eta < 5.0$, respectively, thus resulting a $|\Delta\eta| > 2$ gap. Either $\pi^{\pm}$, $\mathrm{K}^{\pm}$, and $\mathrm{p}+\overline{\mathrm{p}}$ are taken as POI from a p_{T} interval, while inclusive charged particles with $0.2 < p_{\mathrm{T}} < 3.0$ GeV/c are chosen as RPs. The v_2 coefficient is

measured in seven multiplicity classes defined as fractions of the analyzed event sample, based on charged particles with $-5.0 < \eta < -3.0$ and $0.2 < p_{\mathrm{T}} < 3.0$ GeV/c, and denoted 0–5%, 5–10%, 10–20%, 20–40%, 40–60%, 60–80%, 80–100% from the highest to the lowest multiplicity.

The second order two- ($c_2\{2\}$) and four-particle ($c_2\{4\}$) cumulants are extracted using the cumulant method [14, 15]. They are calculated for unidentified charged particles as

$$c_2\{2\} = \langle\langle 2\rangle\rangle, \tag{2}$$

$$c_2\{4\} = \langle\langle 4\rangle\rangle - 2 \cdot \langle\langle 2\rangle\rangle. \tag{3}$$

with $\langle 2\rangle$ and $\langle 4\rangle$ given by

$$\langle 2\rangle = \frac{|Q_n|^2 - M}{M(M-1)}, \tag{4}$$

$$\langle 4\rangle = \frac{|Q_n|^4 + |Q_{2n}|^2 - 2 \cdot \mathfrak{Re}\left[Q_{2n}Q_n^*Q_n^*\right]}{M(M-1)(M-2)(M-3)} - 2\,\frac{2(M-2)\cdot|Q_n|^2 - M(M-3)}{M(M-1)(M-2)(M-3)}.$$

3. Results

Figure 1 presents the p_{T}−differential v_2 of $\pi^{\pm}$, $\mathrm{K}^{\pm}$, and p+$\overline{\mathrm{p}}$ for $|\Delta\eta| > 1.0$ gap for various multiplicity classes from PYTHIA8 Monash tune (left) and rope hadronization (middle), and EPOS4 (right) simulations of pp collisions at $\sqrt{s} = 13.6$ TeV. Its magnitude increases with p_{T} and multiplicity class. Except the 0–5% multiplicity class of EPOS4, the mass ordering (i.e., lighter particles have a larger v_2 than heavier particles at the same p_{T}) is broken. In addition, no grouping into mesons and baryons is observed at intermediate p_{T} for all investigated multiplicity classes.

The p_{T}−differential v_2 of $\pi^{\pm}$, $\mathrm{K}^{\pm}$, and p+$\overline{\mathrm{p}}$ for $|\Delta\eta| > 2.0$ gap for various multiplicity classes from different PYTHIA8 and EPOS4 configurations of pp collisions at $\sqrt{s} = 13.6$ TeV is shown in Fig. 2. A mass ordering is observed at low transverse momentum in the range $0.2 < p_T < 2.0$ GeV/c for the 0–5% and 20–40% multiplicity classes, while it is broken for the 60–80% multiplicity class. The v_2 from the Rope hadronization mode of PYTHIA8 exhibits a stronger mass ordering than that from Monash tune. The p+$\overline{\mathrm{p}}$ v_2 crosses and is higher than that of $\pi^{\pm}$ at intermediate p_{T} for Monash tune. However, no particle type grouping is exhibited by any PYTHIA8 and EPOS4 modes.

Figure 3 shows the v_2 of identified particles for $|\Delta\eta| > 1$ (top) and $|\Delta\eta| > 2$ (bottom) gaps for different multiplicity classes of p–Pb collisions at $\sqrt{s_{\mathrm{NN}}} = 5.02$ TeV generated with PYTHIA8 Angantyr model. The mass ordering is broken for $|\Delta\eta| > 1$, resembling the behavior observed in pp collisions. For $|\Delta\eta| > 2$, the particles are weakly mass-ordered at low p_{T} and a crossing between p+$\overline{\mathrm{p}}$ and $\pi^{\pm}$ v_2 is observed at intermediate p_{T}.

The second order two- ($c_2\{2\}$) and four-particle ($c_2\{4\}$) cumulants of unidentified charged particles as a function of charged particle multiplicity from PYTHIA8 Monash tune and Rope hadronization and EPOS4 core+corona+hadronic rescattering are presented in Fig. 4. Different $|\Delta\eta|$ gaps are applied to suppress nonflow contributions. The $c_2\{2\}$ is positive and decreases with multiplicity and $|\Delta\eta|$ gap, while the $c_2\{4\}$ is consistent with zero at high multiplicity and over the entire multiplicity range when a $|\Delta\eta|$ gap is introduced. These trends are qualitatively similar for all PYTHIA8 and EPOS4 modes. More details can be found in Refs. [16, 17].

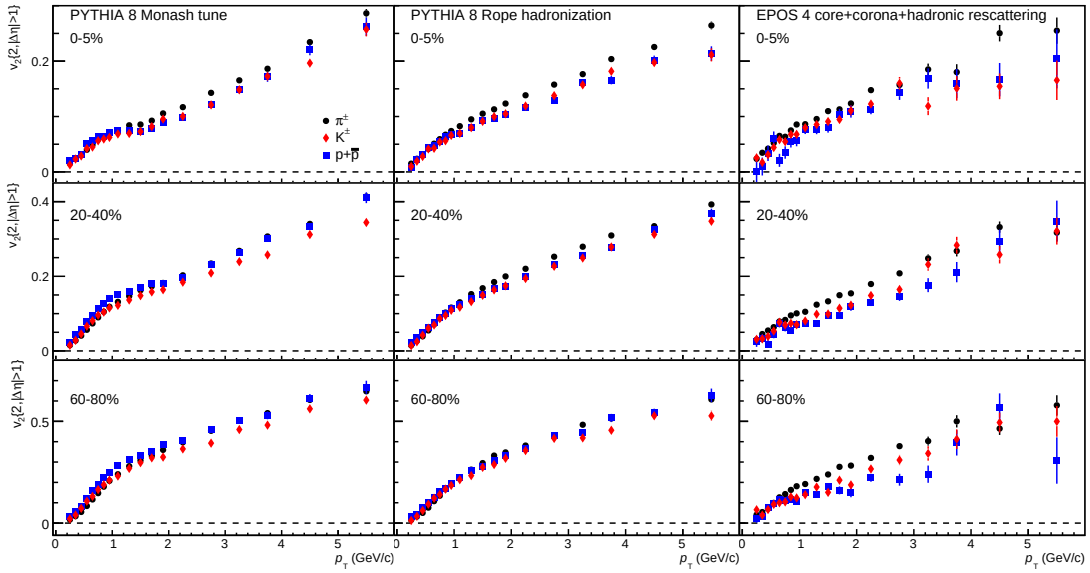

Figure 1: The p_{T}−differential $v_2\{2\}$ of $\pi^{\pm}$, $\mathrm{K}^{\pm}$, and p+$\bar{\mathrm{p}}$ for $|\Delta\eta| > 1$ gap in the 0–5% (top), 20–40% (middle), and 60–80% (bottom) multiplicity classes from different PYTHIA8 and EPOS4 configurations of pp collisions at $\sqrt{s}$ = 13.6 TeV.

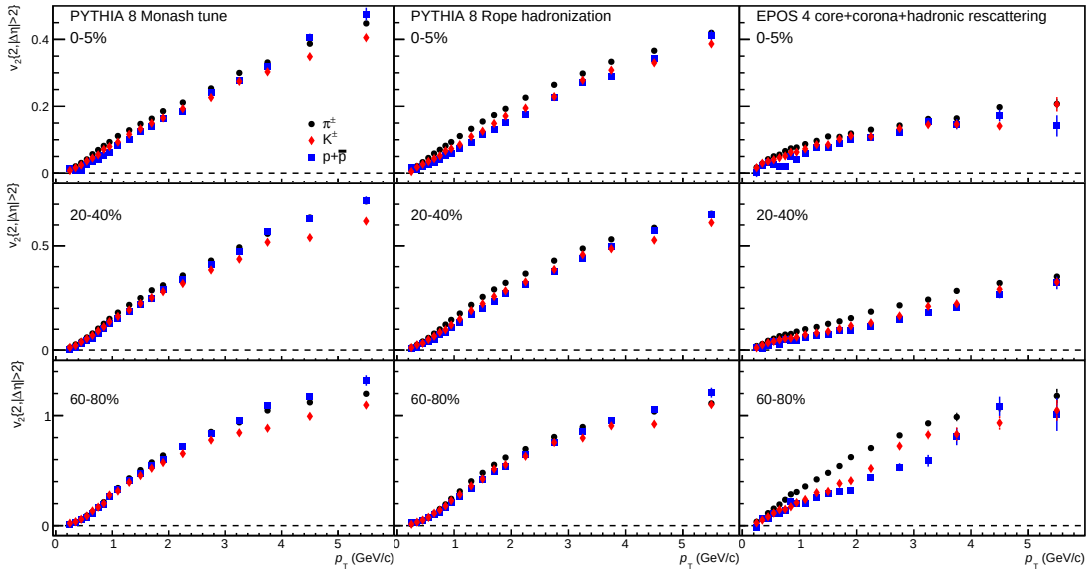

Figure 2: The p_{T}−differential $v_2\{2\}$ of $\pi^{\pm}$, $\mathrm{K}^{\pm}$, and p+$\bar{\mathrm{p}}$ for $|\Delta\eta| > 2$ gap in the 0–5% (top), 20–40% (middle), and 60–80% (bottom) multiplicity classes from different PYTHIA8 and EPOS4 configurations of pp collisions at $\sqrt{s}$ = 13.6 TeV.

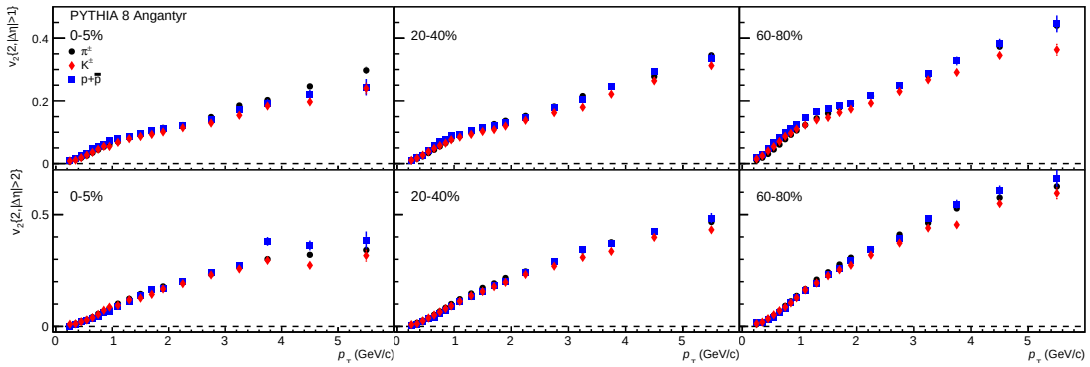

Figure 3: The p_{T}−differential $v_2\{2\}$ of $\pi^{\pm}$, $\mathrm{K}^{\pm}$, and p+$\overline{\mathrm{p}}$ for $|\Delta\eta| > 1$ (top) and $|\Delta\eta| > 2$ (bottom) gaps in the 0–5% (left), 20–40% (middle), and 60–80% (right) multiplicity classes from PYTHIA8 Angantyr model of p–Pb collisions at $\sqrt{s_{\mathrm{NN}}} = 5.02$ TeV.

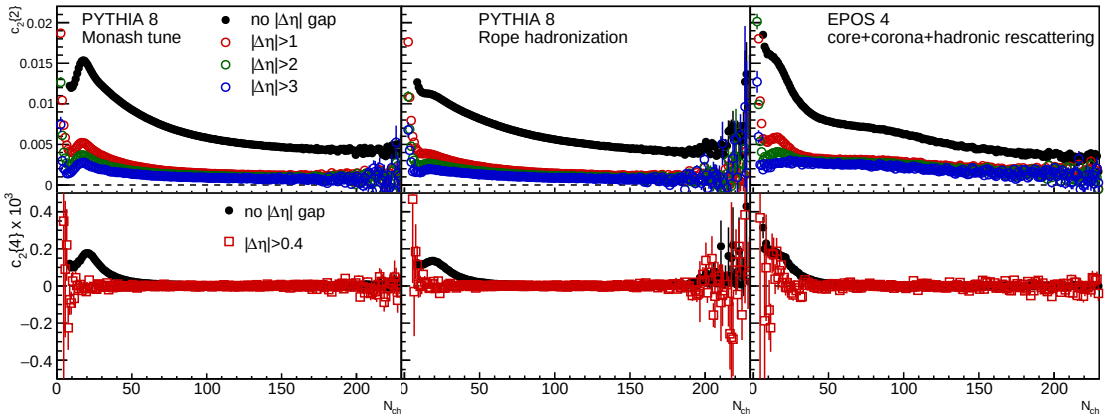

Figure 4: $c_2\{2\}$ (top) and $c_2\{4\}$ (bottom) as a function of charged-particle multiplicity from different PYTHIA8 and EPOS4 configurations of pp collisions at $\sqrt{s} = 13.6$ TeV.

4. Summary

In order to investigate collective effects in small collision systems, the study was centered on the second order Fourier coefficient and the two- and four-particle cumulants in pp and p–Pb collisions generated by PYTHIA8 and EPOS4. For a $|\Delta\eta| > 2$ gap introduced to suppress nonflow contributions, the mass ordering is visible in all configurations, being more pronounced for Rope hadronization. A crossing between p+$\overline{\mathrm{p}}$ and $\pi^{\pm}$ v_2 at intermediate p_{T} is observed for PYTHIA8 Monash tune of pp collisions and Angantyr model of p–Pb collisions. The second order two- and four-particle cumulants behave qualitatively similar for PYTHIA8 and EPOS4. The $c_2\{2\}$ decreases with multiplicity and $|\Delta\eta|$ gap, while $c_2\{4\}$ is consistent with 0 when a $|\Delta\eta|$ gap is applied.

Acknowledgments

This research was supported by a grant of the Ministry of Research, Innovation and Digitization, CNCS – UEFISCDI, project number PN-III-P4-PCE-2021-0390, within PNCDI III.

References

[1] V. Khachatryan *et al.* [CMS], JHEP **09** (2010), 091.

[2] B. Abelev *et al.* [ALICE], Phys. Lett. B **719** (2013), 29-41.

[3] K. Aamodt *et al.* [ALICE], Phys. Rev. Lett. **105** (2010), 252302.

[4] S. Voloshin and Y. Zhang, Z. Phys. C **70** (1996), 665-672.

[5] B. B. Abelev *et al.* [ALICE], Phys. Lett. B **726** (2013), 164-177.

[6] V. Khachatryan *et al.* [CMS], Phys. Lett. B **765** (2017), 193-220.

[7] K. Werner, Phys. Rev. C **108** (2023) no.6, 064903.

[8] C. Bierlich *et al.* SciPost Phys. Codeb. **2022** (2022), 8.

[9] B. Andersson, G. Gustafson, G. Ingelman and T. Sjostrand, Phys. Rept. **97** (1983), 31-145.

[10] C. Bierlich, G. Gustafson, L. Lönnblad and A. Tarasov, JHEP **03** (2015), 148.

[11] P. Skands, S. Carrazza and J. Rojo, Eur. Phys. J. C **74** (2014) no.8, 3024.

[12] C. Bierlich, G. Gustafson, L. Lönnblad and H. Shah, JHEP **10** (2018), 134.

[13] C. Adler *et al.* [STAR], Phys. Rev. C **66** (2002), 034904.

[14] A. Bilandzic, R. Snellings and S. Voloshin, Phys. Rev. C **83** (2011), 044913.

[15] J. Jia, M. Zhou and A. Trzupek, Phys. Rev. C **96** (2017) no.3, 034906.

[16] A. Manea, A. F. Dobrin, A. Danu and C. D. Brandibur, PoS **EPS-HEP2023** (2024), 203.

[17] D. C. Brandibur, A. Danu, A. F. Dobrin and A. Manea, PoS **EPS-HEP2023** (2024), 282.